Article

Speciation of Technetium Dibutylphosphate in the Third Phase Formed in the TBP/HNO$_3$ Solvent Extraction System

Jonathan George, Ramsey Salcedo, Rachel Greenberg, Hossam Elshendidi, Donna McGregor, Benjamin Burton-Pye, Lynn C. Francesconi, Alena Paulenova, Artem V. Gelis, and Frederic Poineau*

Read Online

ACCESS | Metrics & More | Article Recommendations | Supporting Information

ABSTRACT: The speciation of technetium in the nitric acid/dibutylphosphoric acid (HDBP)—*n*-dodecane system was studied by extended X-ray absorption fine structure (EXAFS) spectroscopy and theoretical methods. Tetravalent technetium, produced by the hydrazine reduction of TcO$_4^-$ in 3 M HNO$_3$, was extracted by HDBP in *n*-dodecane (30% by volume). During extraction, the splitting of the organic phase into a heavy phase and a light phase was observed. EXAFS analysis is consistent with the presence of Tc(NO$_3$)$_3$(DBP)-(HDBP)$_2$ in the light phase and Tc(NO$_3$)$_2$(DBP)$_2$(HDBP)$_2$ in the heavy phase. Density functional theory calculations at the B3LYP/6-31G* level confirm the stability of the proposed species and indicate that stereoisomers -mer- and fac-Tc(NO$_3$)$_3$(DBP)(HDBP)$_2$ for the light phase and cis- and trans-Tc(NO$_3$)$_2$(DBP)$_2$(HDBP)$_2$ for the heavy phase] could coexist in the system (in the *n*-dodecane solution). Mechanisms of formation of Tc(NO$_3$)$_3$(DBP)(HDBP)$_2$ and Tc(NO$_3$)$_2$(DBP)$_2$(HDBP)$_2$ are proposed.

Technetium - third phase
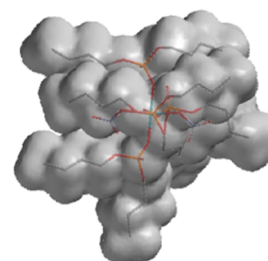
Tc(NO$_3$)$_2$(DBP.HDBP)$_2$

INTRODUCTION

First reported by Segrè and Seaborg in 1938,[1] the isotope ^{99}Tc (β_{max} = 294 keV; $T_{1/2}$ = 2.1 × 10^5 y) is one of the major fission products found in the spent nuclear fuel (SNF) (fission yield ~6.1% from ^{235}U).[2] Due to a long half-life and beta radiotoxicity, ^{99}Tc represents a hazard for the management of SNF. Several options for SNF management are considered, one of them being the mutual recovery of U and Pu using advanced separation processes.[3,4] Most of these processes are based on solvent extraction of U and Pu from the SNF dissolved in nitric acid with tributylphosphate [(TBP, C$_4$H$_9$O)$_3$PO] in an organic phase. In some recently proposed processes, strong reducing agents such a mixture of U(IV) and hydrazine are used for Pu striping.[4]

In these processes, ^{99}Tc technetium poses problems as it follows the U and Pu streams.[5]

Under the process conditions, a considerable amount of Tc, typically present as the pertechnetate anion Tc^{VII}O$_4^-$, may reduce and form a cation of Tc(IV). It was proposed that the dibutylphosphoric acid [HDBP, (C$_4$H$_9$O)$_2$(OH)PO], a primary degradation product of TBP, forms a Tc(IV)-dibutylphosphate species, providing a route for Tc to enter the Pu stream.[6] In such a way, HDBP has an antagonistic effect on several separation operations[7] as it forms strong complexes also with actinides and inhibits their stripping from the organic phase.[8] It can lead to precipitation of metal complexes[9] and promote the formation of a "third phase"[10] that can disrupt separation operations.

In solvent extraction, the "third phase" phenomenon is observed when the postextraction organic phase divides into two phases of different densities (i.e., a light phase and a heavy phase).[11,12] The light phase contains low concentrations of the extracted metal complex (and the coextracted aqueous acid and its anion), while the heavy phase (the "third phase") contains high concentrations of the extracted metal complexes, acid, and extracting agent. In SNF processing, it is essential to avoid third phase formation to prevent the accumulation of fissile isotopes (i.e., ^{239}Pu) that can potentially lead to criticality conditions. Additionally, two organic phases prohibit accurate separation in centrifugal extractors. The third phase formation have been well documented for the M-HNO$_3$/TBP-alkane systems (M = Th,[13] U,[14] Np,[15] Pu,[16] Zr,[17] and Ce[18]), while the studies on the M-HNO$_3$/HDBP-alkane systems (M = Zr,[10] Tc,[6] and Eu[19]) are scarce.

For the Tc(IV)-HNO$_3$/HDBP-dodecane system, we have shown that the extraction of Tc(IV) from 0.5 M HNO$_3$ with TBP/DBP (15%/15% by volume) in *n*-dodecane produced a single organic phase that contains the Tc(NO$_3$)$_3$(DBP) species.[20] Because it does not extract Tc(IV), TBP does not affect the speciation of Tc(IV) in the organic phase after extraction. Boukis et al. have shown that during extraction with HDBP >20 vol %, a third phase occurred, but the speciation of Tc in the third phase was not reported.[6] The acquisition of

speciation data in the third phase formed in the Tc(IV)-HNO$_3$ /HDBP-dodecane system is essential to comprehend the chemistry of Tc during the SNF processing and develop chemical models that can be used to simulate the behavior of Tc in advance separation processes.

Here, we performed UV−visible spectroscopy, X-ray absorption near-edge spectroscopy (XANES), and extended X-ray absorption fine structure (EXAFS) spectroscopy to analyze the extraction system of Tc(IV) in 3 M HNO$_3$ /HDBP-dodecane (30 vol %) and elucidate the speciation of Tc(IV) in the light and heavy organic phases formed during the extraction process. The species suggested by EXAFS spectroscopy were further analyzed by theoretical methods, and their formation mechanisms were proposed.

■ RESULTS AND DISCUSSION

The extraction of Tc(IV) with HDBP (30 vol %) in *n*-dodecane from 3 M HNO$_3$ was performed (see the Materials and Methods section). Under these concentration conditions, the third phase was formed and the splitting of the organic phase into a heavy phase (sample H) and a light phase (sample L) was observed. Sample H and sample L were analyzed by UV−visible spectroscopy, XANES, and EXAFS spectroscopy. The similarity of the UV−visible spectra (Figure S1) indicates the speciation of Tc in those samples to be related and the concentration of Tc in the heavy phase to be an order of magnitude higher than the one in the light phase.

The XANES spectrum of sample H (Figure S2) exhibits a pre-edge at 21045 eV (1s → 4d dipole forbidden transition), which clearly indicates the presence of TcO$_4^-$ (20−30%). For sample L, the pre-edge at 21045 eV is much less pronounced than for sample H and indicates TcO$_4^-$ to be a minor species (<10%). The analysis of XANES spectra using the first derivative method indicates an absorption edge at 21055.7 eV for sample L and at 21056.0 eV for sample H, which confirms the presence of an octahedral Tc(IV) complex as the main species in both samples. The presence of pertechnetate is likely due to incomplete reduction and/or reoxidation of Tc(IV) with nitric acid.

The EXAFS spectra of sample H and sample L were averaged, k^3-weighed, and subjected to the Fourier transform (FT) in the 3.5−14 Å^{-1} k range. The FT (Figures 1 and 2) shows two peaks centered at R + Δ ∼1.50 and 3.0 Å. The position of these peaks is similar to the one found previously for Tc(NO$_3$)$_3$(DBP) in the TBP/HDBP/n-dodecane (15%/ 15% v/v).[20] Analogically, it is postulated that samples H and L contain a Tc(IV) monomeric species coordinated to nitrate or DBP anions. In order to evaluate this hypothesis, the EXAFS spectra were fitted using the scattering path calculated in the density functional theory (DFT) optimized structure of Tc(NO$_3$)$_3$(DBP) (Figure 3).

For sample H, three different adjustments were performed considering the presence of Tc^{VII}O$_4^-$ and a Tc^{IV} species coordinated to (i) the DBP ligand (fit 1), (ii) DBP and bidentate nitrate ligands (fit 2), and (iii) DBP and monodentate nitrate ligands (fit 3).

For fit 1, scatterings due to TcO$_4^-$ (Tc-Oa) and to the DBP ligand [Tc-Ob, Tc-Oc, Tc-P single scattering (SS), and Tc-P multiscattering (MS)] were considered.

For fit 2 and fit 3, scatterings due to TcO$_4^-$ (Tc-Oa), the DBP ligand [Tc-Ob, Tc-Oc, Tc-P(SS) and Tc-P (MS)], and the nitrate ligand (Tc-Od and Tc-N) were considered.
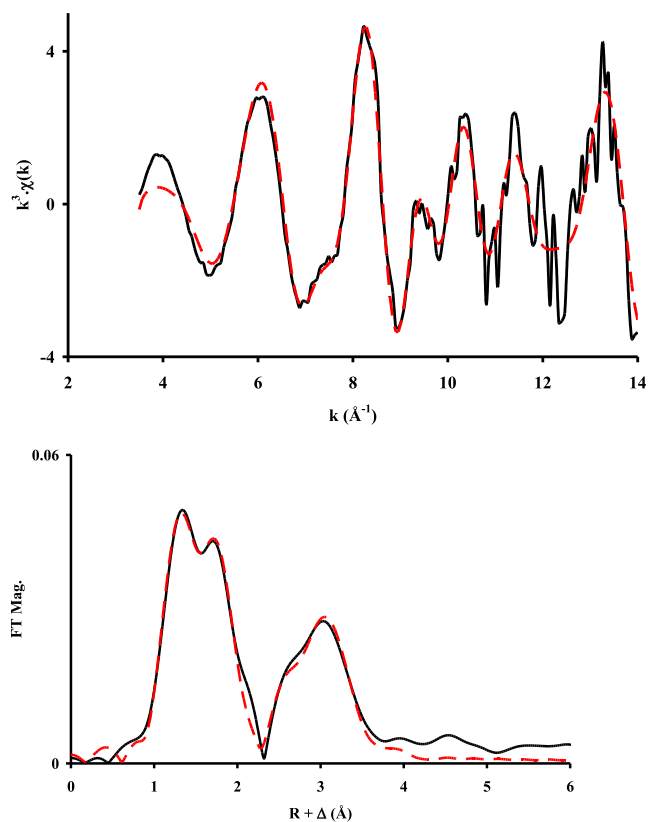
Figure 1. Fitted k^3-EXAFS spectra (top) and FT (bottom) of the k^3-EXAFS spectrum of sample H. Adjustment between k = 3.5 and 14 Å^{-1}. Experimental data are in black and the fit is in red dots.

For all fits, the values of the DWF factor were fixed to 0.002 Å^2 for Tc-Oa, Tc-Ob, Tc-Od, and Tc-N, 0.003 Å^2 for Tc-P(SS), 0.005 Å^2 for Tc-Oc, and 0.006 Å^2 for Tc-P(MS). The following correlation between the coordination numbers (CNs) for Tc-P(SS), Tc-P(MS), and Tc-Oc(DBP) scatterings was used: (CN)$_{Tc-Oc(DBP)}$ = 2 (CN)$_{Tc−P(SS)}$ and (CN)$_{Tc-P(MS)}$ = 2(CN)$_{Tc-P(SS)}$. The value of the reduced-chi^2 for fits 1, 2, and 3 are, respectively, 67.05, 14.01, and 9.99, which indicates the model consisting of monodentate nitrate and DBP ligands (fit 3) to be the most probable.

Results of fit 3 (Figure 1 and Table 1) indicate the presence of 1.2(3) Oa atoms at 1.71(2) Å, 2.8(7) Ob atoms at 2.11(2) Å, 4.8 ± 1.2 Oc atoms at 3.85(4) Å, 0.9(2) Od atoms at 1.93(2) Å, 1.1(3) N atoms at 2.86(3) Å, and 2.4(6) P atoms at 3.39(3) Å.

Sample L was analyzed using a similar approach to the analysis of sample H with the difference that the Tc-Oa scattering was not considered [TcO$_4^-$ being not in a significant amount (<10%) in the sample, vide infra XANES studies]. The results of fitting (Figure 2 and Table 2) indicate the presence of 2.1(5) Ob atoms at 2.14(2) Å, 4.6 ± 1.2 Oc atoms at 3.77(4) Å, 2.9(7) Od atoms at 2.02(2) Å, 2.0(5) N atoms at 2.82(3) Å, and 2.3(6) P atoms at 3.32(3) Å.

The Tc−N distance in samples H and L [i.e., 2.86(3) and 2.82(3) Å] is well consistent with the presence of monodentate nitrate and compares well with the M−N distance found by X-ray diffraction for species containing the monodentate nitrate ligand (Table 3).

For samples H and L, EXAFS analysis indicates the presence of a Tc(IV) monomeric species coordinated to DBP and/or
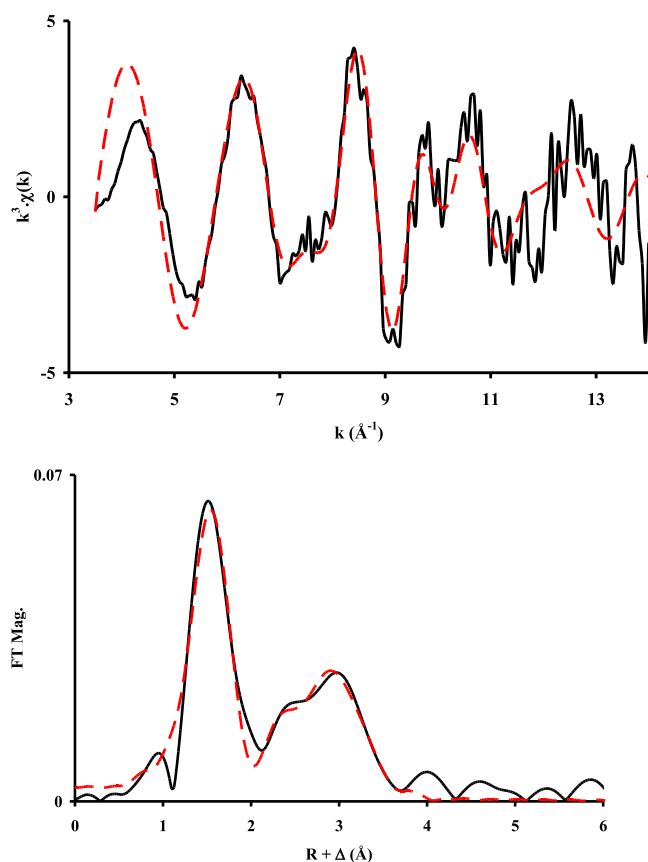
Figure 2. Fitted k^3-EXAFS spectra (top) and FT (bottom) of the k^3-EXAFS spectrum of sample L. Adjustment between k = 3.5 and 14 $Å^{-1}$. Experimental data are in black and the fit is in red dots.
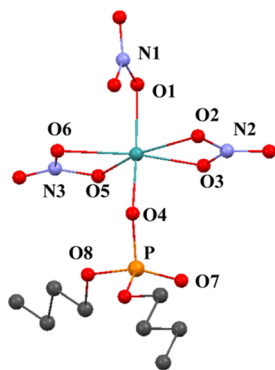
Figure 3. Ball and stick representation of the DFT optimized structure of $Tc(NO_3)_3(DBP)$ used for EXAFS analysis. Selected distances (Å): Tc–O1:2.077, Tc–O2:2.197, Tc–O3:2.043, Tc–O4:1.921, Tc–O5:2.046, Tc–O6:2.213, Tc–N1:2.696, Tc–N2:2.566, Tc–N3:2.576, Tc–P: 3.248, Tc–O7:3.772, and Tc–O8:3.662. Color of atoms: Tc in blue, O in red, C in gray, N in purple, and P in orange. H atoms are omitted for clarity.

Table 1. EXAFS Fit Parameters Obtained by the Fit of the k^3-EXAFS Spectra for Sample H[a]

scattering path	C.N	R (Å)	σ^2 (Å^2)
Tc-Oa(TcO4)	1.2 ± 0.3	1.71(2)	0.002[b]
Tc-Ob(DPP)	2.8 ± 0.7	2.11(2)	0.002[b]
Tc-Oc(DBP)	4.8 ± 1.2[c]	3.85(4)	0.005[b]
Tc-Od(NO3)	0.9 ± 0.2	1.93(2)	0.002[b]
Tc–N(NO3)	1.1 ± 0.3	2.86(3)	0.002[b]
Tc–P(SS)	2.4 ± 0.6[c]	3.39(3)	0.003[b]
Tc–P(MS)	4.8 ± 1.2[c]	3.67(4)	0.006[b]

[a]ΔE_0 = 1.83 eV. Reduced-chi^2: 9.99. Residual = 5.59%. [b]Fixed parameter. [c]Correlated parameter. SS: single scattering. MS: multi-scattering.

Table 2. EXAFS Fit Parameters Obtained by the Fit of the k^3-EXAFS Spectra for Sample L[a]

scattering path	C.N	R (Å)	σ^2 (Å^2)
Tc-Ob(DBP)	2.1 ± 0.5	2.14(2)	0.002[b]
Tc-Oc(DBP)	4.6 ± 1.2[c]	3.77(4)	0.005[b]
Tc-Od(NO3)	2.9 ± 0.7	2.02(2)	0.002[b]
Tc–N(NO3)	2.0 ± 0.5	2.82(3)	0.002[b]
Tc–P(SS)	2.3 ± 0.6[c]	3.32(3)	0.003[b]
Tc–P(SS)	2.3 ± 0.6[c]	3.32(3)	0.003[b]

[a]ΔE_0 = 1.28 eV. Reduced-chi^2: 49.41. R = 11.96%. [b]Fixed parameter. [c]Correlated parameter.

Table 3. Interatomic M–N Distances (Å) Found by X-Ray Diffraction in Species Containing Nitrate Ligands Coordinated in Monodentate (M–N$_{mono}$) and Bidentate (M–N$_{bid}$) Modes

species	M–Nmono	M–Nbid
$Cs_2[Rh(NO_3)_5]$[21]	2.896–2.909	2.448
$[Ru(C_{10}H_{16})Cl(NO_3)]$[22]		2.594
$[Ru(C_{10}H_{16})(NO_3)_2]$[3]	2.757	
$[RuNO(Py)_2(NO_3)_3]$[23]	2.956–2.990	
$(NO)_2[Pt(NO_3)_6]$[24]	2.916–2.944	
$Cs[MoO_2(NO_3)_3]$[25]	2.977–3.062	2.743
$[MoO_2(NO_3)_2]$[25]		2.615–2.602
$Cs[VO_2(NO_3)_2]_3$[25]	2.824–2.857	

sample H and $Tc(NO_3)_3(DBP)(HDBP)_2$ for sample L. For sample H, the metal to ligand ratio (Tc: DBP) found by EXAFS (1:4) is in agreement with the one found previously by slope analysis (1:4).[6] It is likely that a difference of the HDBP concentration in the light and heavy phases is the origin of the difference of Tc(IV) speciation in both phases. The stoichiometries $M(NO_3)_2(DBP)_2(HDBP)_2$ and $M(NO_3)_3(DBP)(HDBP)$ have already been reported for Zr species using electrospray ionization mass spectrometry.[27] Additionally, $Zr(NO_3)_2(DBP)_2(HDBP)_2$ was reported during the extraction of Zr(IV) in 2 M HNO_3 with HDBP in toluene.[28]

The structure of $Tc(NO_3)_2(DBP)_2(HDBP)_2$ and $Tc(NO_3)_3(DBP)(HDBP)_2$ stereoisomers was studied by the DFT method. The atomic coordinates for the structures are provided in the Supporting Information. For $Tc(NO_3)_2(DBP)_2(HDBP)_2$, cis-$Tc(NO_3)_2(DBP)_2(HDBP)_2$ (complex A) and trans-$Tc(NO_3)_2(DBP)_2(HDBP)_2$ (complex B), which, respectively, contain nitrate ligands in cis and trans positions, were considered. For $Tc(NO_3)_3(DBP)(HDBP)_2$, the following stereoisomers were considered: mer-Tc-

HDBP ligands and to the monodentate nitrate ligand. Because the species in the organic phase exhibit a neutral charge,[26] the stoichiometry $(Tc(NO_3)_x)(DBP)_y(HDBP)_z$ is proposed. In order to determine the values of x, y, and z for both samples, the atomic ratios (O/P, O/N, and P/N) found by EXAFS were compared to the one in theoretical species that fulfilled the conditions $x + y = 4$ (species with a neutral charge) and $x + y + z = 6$ (species hexacoordinated). The results (Table 4) are consistent with the presence of $Tc(NO_3)_2(DBP)_2(HDBP)_2$ for

Table 4. Atomic Ratios O/P, O/N, and P/N Found Theoretically in Tc(NO$_3$)$_2$(DBP)$_2$(HDBP)$_2$ and Tc(NO$_3$)$_3$(DBP)(HDBP)$_2$ and Found by EXAFS in Sample H and Sample L

	O/P	O/N	P/N
sample H	1.54 ± 0.54	3.36 ± 1.19	2.18 ± 0.77
sample L	2.17 ± 0.77	2.50 ± 0.88	1.15 ± 0.41
Tc(NO$_3$)$_2$(DBP)$_2$(HDBP)$_2$	1.50	3.00	2.00
Tc(NO$_3$)$_3$(DBP)(HDBP)$_2$	2.00	2.00	1.00

(NO$_3$)$_3$(DBP)(HDBP)$_2$ (complex C) and (fac-Tc-(NO$_3$)$_3$(DBP)(HDBP)$_2$) (complex D), which, respectively, contain the nitrate ligands in the meridian and facial position. Additionally, Tc(NO$_3$)$_3$(DBP) (Figure 3) was studied. Theoretical calculations confirm the stability of the proposed complexes, and their optimized structures are presented in Figure 4. The distances found by DFT (Table 5) are in good
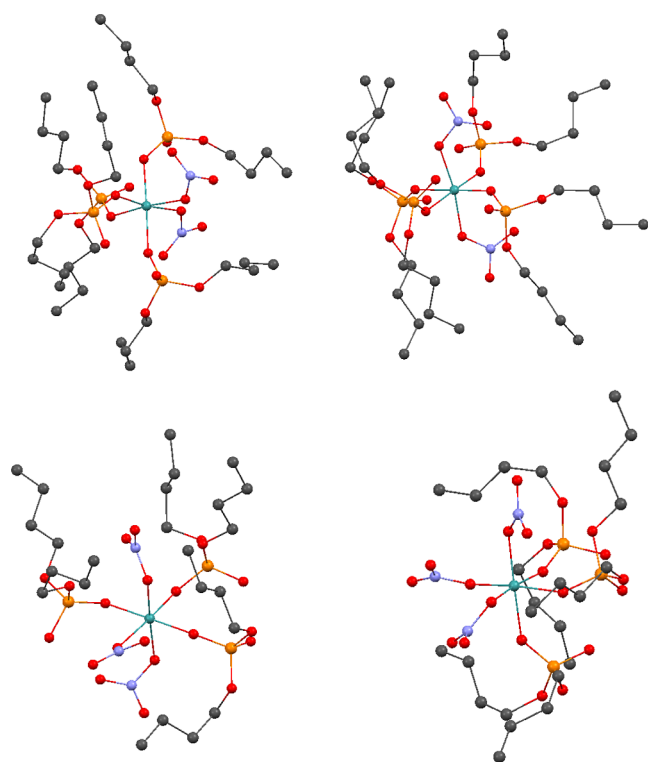
Figure 4. Ball and stick representation of the DFT optimized structure of cis-Tc(NO$_3$)$_2$(DBP)$_2$(HDBP)$_2$ (top-left), trans-Tc-(NO$_3$)$_2$(DBP)$_2$(HDBP)$_2$ (top-right), mer-Tc(NO$_3$)$_3$(DBP)(HDBP)$_2$ (bottom-left), and fac-Tc(NO$_3$)$_3$(DBP)(HDBP)$_2$ (bottom-right). Color of atoms: Tc in blue, O in red, C in gray, N in purple, and P in orange. H atoms are omitted for clarity.

agreement with the experimental XAFS results. Energetic calculations indicate a difference of 36.14 kJ/mol between complexes A and B and 17.97 kJ/mol between complexes C and D. These results indicate that complexes A and C could, respectively, coexist in solution with complexes B and D.

The energy separation (HOMO−LUMO gap) between the highest occupied molecular orbital (HOMO) and the lowest unoccupied molecular orbital (LUMO) has been calculated. The HOMO−LUMO gap has been used as an indicator of the kinetic stability of Tc complexes.[29] For complex A, B, C, and D, the HOMO−LUMO gap is between 3.45 and 3.58 eV, which indicates that these complexes have similar kinetic stability. It is noted that the HOMO−LUMO gap for complexes C and D (3.45 and 3.46 eV, respectively) is larger than the one for Tc(NO$_3$)$_3$(DBP) (2.93 eV), which emphasizes the stabilizing effect of the HDBP molecule.

Finally, the calculated spectra for complexes A, B, C, and D exhibit maximum absorption bands, respectively, at 380, 403, 418, and 442 nm (Figure S3). The calculated spectra are in agreement with the experimental spectra of the light and heavy phases (figure S1) and support the presence of these complexes in solution.

Our results confirm that the third phase formation in the Tc(IV)-HNO$_3$/HDBP-n-dodecane system is dependent on the HDBP concentration in the organic phase. For extraction with TBP/HDBP(15v %/15v %) in n-dodecane, third phase formation was not observed and the speciation is dominated by Tc(NO$_3$)$_3$(DBP), while for 30% /HDBP in dodecane, third phase formation occurred with the presence of Tc-(NO$_3$)$_2$(DBP)$_2$(HDBP)$_2$ in the heavy phase and Tc-(NO$_3$)$_3$(DBP)(HDBP)$_2$ in the light phase.

In order to explain these speciation results, the Tc(IV)-HNO$_3$−HDBP system was compared to the Zr(IV)-HNO$_3$−HDBP system. Upon extraction of Zr(IV) with HDBP from HNO$_3$, the Zr(NO$_3$)$_3$(DBP) (eq 1) and Zr-(NO$_3$)$_2$(DBP)$_2$(HDBP)$_2$ (eq 2) species can be formed in the organic phase and the speciation depends on the Zr:HDBP ratio.[9,28,30] It was proposed that the species in the third phase (i.e., Zr(NO$_3$)$_2$(DBP)$_2$) was formed from the reaction of Zr(NO$_3$)$_3$(DBP) with HDBP (eq 3).[31]

Table 5. Calculated HOMO−LUMO Gap (ΔE in eV) and Average Tc−O(DBP), Tc−O(NO3), Tc−N, and Tc−P Interatomic Distance (Å) in the Optimized Structure of cis-Tc(NO$_3$)$_2$(DBP)$_2$(HDBP)$_2$, trans-Tc(NO$_3$)$_2$(DBP)$_2$(HDBP)$_2$, mer-Tc(NO$_3$)$_3$(DBP)(HDBP)$_2$, fac-Tc(NO$_3$)$_3$(DBP)(HDBP)$_2$, and Tc(NO$_3$)$_3$(DBP)

species	Tc−O(P)	Tc−O(N)	Tc−N	Tc−P	ΔE
cis-Tc(NO$_3$)$_2$(DBP)$_2$(HDBP)$_2$	2.002	2.037	3.058	3.315	3.58
trans-Tc(NO$_3$)$_2$(DBP)$_2$(HDBP)$_2$	2.002	2.040	3.041	3.339	3.46
mer-Tc(NO$_3$)$_3$(DBP)(HDBP)$_2$	2.004	2.037	3.049	3.317	3.45
fac-Tc(NO$_3$)$_3$(DBP)(HDBP)$_2$	2.047	1.996	2.993	3.374	3.46
Tc(NO$_3$)$_3$(DBP)	1.921	2.115	2.696[a]	3.248	2.93
			2.571		

[a]Monodentate.

$$Zr^{4+} + 3NO_3^- + HDBP \rightarrow Zr(NO_3)_3(DBP)_{org} + H^+ \quad (1)$$

$$Zr^{4+} + 2NO_3^- + 4HDBP$$
$$\rightarrow Zr(NO_3)_2(DBP)_2(HDBP)_2 + 2H^+ \quad (2)$$

$$Zr(NO_3)_3(DBP)_{org} + 2HDBP$$
$$\rightarrow Zr(NO_3)_2(DBP)_2 + HNO_3 \quad (3)$$
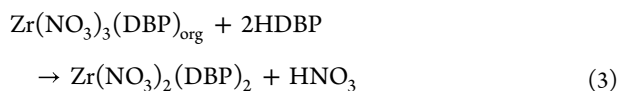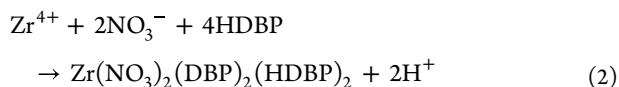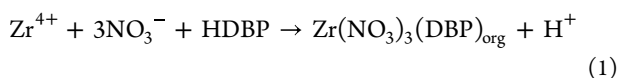
For the Tc(IV)-HNO$_3$/HDBP-dodecane system, we propose that Tc(IV) is extracted with HDBP/TBP (15/15 vol %) as Tc(NO$_3$)$_3$(DBP) (eq 4) without third phase formation. When Tc(IV) is extracted with 30%v HDBP, we propose that Tc(IV) is initially extracted as Tc(NO$_3$)$_3$(DBP)(HDBP)$_2$ (eq 5), which further reacts with HDBP and forms Tc-(NO$_3$)$_2$(DBP)$_2$(HDBP)$_2$ (eq 6). The overall formation mechanism of Tc(NO$_3$)$_2$(DBP)$_2$(HDBP)$_2$ (eqs 7 and 8) obtained by combining eqs 5 and 6 is similar to the one of Zr(NO$_3$)$_2$(DBP)$_2$(HDBP) (eq 2). By comparison with the Zr(IV)-HNO$_3$/TBP-octane system,[32] we suggest that the aggregation of Tc(NO$_3$)$_2$(DBP)$_2$(HDBP)$_2$ into primary and supramolecular clusters is the origin of the third phase formation.

$$Tc^{4+} + 3NO_3^- + HDBP \rightarrow Tc(NO_3)_3(DBP)_{org} + H^+ \quad (4)$$

$$Tc^{4+} + 3NO_3^- + 3HDBP$$
$$\rightarrow Tc(NO_3)_3(DBP)(HDBP)_2 + H^+ \quad (5)$$

$$Tc(NO_3)_3(DBP)(HDBP)_2 + HDBP$$
$$\rightarrow Tc(NO_3)_2(DBP)_2(HDBP)_2 + HNO_3 \quad (6)$$

$$Tc^{4+} + 2NO_3^- + 4HDBP + HNO_3$$
$$\rightarrow Tc(NO_3)_2(DBP)_2(HDBP)_2 + HNO_3 + 2H^+ \quad (7)$$

$$Tc^{4+} + 2HNO_3 + 4HDBP$$
$$\rightarrow Tc(NO_3)_2(DBP)_2(HDBP)_2 + 4H^+ \quad (8)$$
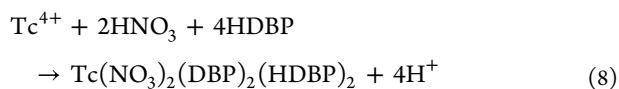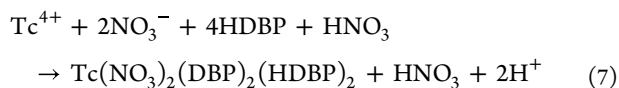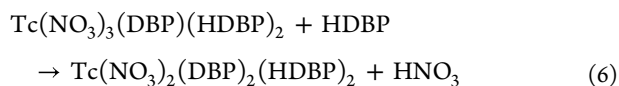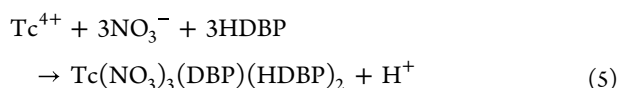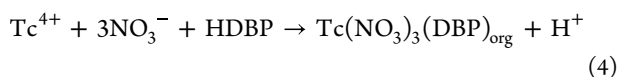
■ CONCLUSIONS

In summary, Tc(IV) produced from the reduction of TcO$_4^-$ in nitric acid by hydrazine was extracted by HDBP (30% by volume) in n-dodecane. Following extraction, splitting of the organic phase into a heavy phase and a light phase was observed. The Tc concentration in the heavy phase was found to be an order of magnitude higher than that in the light phase. EXAFS analysis is consistent with the presence of Tc-(NO$_3$)$_3$(DBP)(HDBP)$_2$ in the light phase and Tc-(NO$_3$)$_2$(DBP)$_2$(HDBP)$_2$ in the heavy phase. Theoretical calculations confirm the stability of the proposed complexes and indicate that stereoisomers could coexist in solution. The mechanisms of extraction and third phase formation were proposed. According to these mechanisms, Tc(IV) is initially extracted in the organic phase as Tc(NO$_3$)$_3$(DBP)(HDBP)$_2$. Tc(NO$_3$)$_3$(DBP)(HDBP)$_2$ reacts with HDBP and forms Tc(NO$_3$)$_2$(DBP)$_2$(HDBP)$_2$, which aggregates into supramolecular clusters and ultimately leads to third phase formation. More studies are needed to confirm these hypothetical mechanisms. The study of third phase formation

in the Tc(IV)-HNO$_3$/HDBP-dodecane system using small-angle neutron scattering could provide structural information on the cluster formed during the aggregation. We also note that the third phase formation could also occur in the Tc(IV)-HNO$_3$/dodecane extraction system that uses other organophosphorus extracting agents, i.e., HDEHP (di(2-ethylhexyl)-phosphoric acid) or HEH[EHP] (2-ethylhexyl phosphoric acid mono 2-ethylhexyl ester).[33,34] So far, Tc(IV)-HDEHP complexes are unknown, but it can be anticipated, by comparison with the HDBP system, that Tc(NO$_3$)$_2$(H(L)$_2$)$_2$ (L = DEHP or EH[EHP]) could be formed in the organic phase following extraction.

■ MATERIALS AND METHODS

Caution! Technetium-99 is a weak beta emitter with E(max) = 292 keV. All manipulations were performed in radiochemistry laboratories designed for chemical synthesis using efficient HEPA-filtered fume hoods and following locally approved radioisotope handling and monitoring procedures.

Materials. The technetium starting material, solid ammonium pertechnetate (NH$_4$TcO$_4$), was purchased from the Oak Ridge National Laboratory. Solid KTcO$_4$ was obtained after the dissolution of NH$_4$TcO$_4$ in water and precipitation with an aqueous KOH solution. A Tc-stock solution (0.107 M) was prepared by dissolving solid KTcO$_4$ in water. HDBP (≥97%, assay 98.4%), n-dodecane, and hydrazine (N$_2$H$_4$, 98%) were obtained from Sigma-Aldrich and used as received. The main impurity in HDBP is TBP (∼2%). Deionized water (18.2 MΩ) was used.

Samples for XAFS Spectroscopy. The sample containing Tc(NO$_3$)$_3$(DBP) was prepared in two steps: first, the hydrazine reduction of heptavalent Tc (TcO$_4^-$) in 3 M HNO$_3$, followed by dilution to 0.5 M HNO$_3$ and extraction with TBP/DBP (15%/15% vol) in dodecane. An aliquot of the KTcO$_4$ stock solution (140 μL) was diluted with 3 M HNO$_3$ (2.676 mL); then, hydrazine (93 μL) was added to make a 3 mL sample, and the vial was left undisturbed. After a day, when this sample turned brown, it was mixed with 3 mL of the HDBP/n-dodecane solution (30% by volume) and agitated (vortexed) for 30 min. The sample was allowed to split, and the resulting organic and aqueous phases were separated. The organic phase contained two layers: a heavy layer at the bottom (sample H) and a light layer at the top (sample L) that were carefully separated with a pipet, collected, and analyzed by UV−visible spectroscopy, XANES, and EXAFS spectroscopy.

The distribution coefficient (DTc) calculated for our system (DTc = 0.364) is in the same range as that for the one previously reported (DTc ≈ 0.5) for a similar system [i.e., Tc(IV), 3 M HNO$_3$, 15% HDBP, and a total Tc concentration of 0.3 mM].[6]

XAFS Measurements. XAFS measurements were performed at the Argonne National Laboratory Advanced Photon Source at the BESSRC-CAT 12 μ$_B$-B station. The technetium sample (∼18 μL) was placed in a Teflon NMR tube insert holder and covered with a Kapton film. XAFS spectra were recorded at the Tc−K edge (21,044 eV) in the fluorescence mode at room temperature using a 13 element germanium detector. A double crystal of Si [1 1 1] was used as a monochromator. The energy steps were 0.6 eV in the XANES region and 0.05 Å^{-1} in the EXAFS region. The energy was calibrated using a molybdenum foil (Mo−K edge = 20,000 eV). Fifteen spectra were recorded in the 0−15 Å^{-1} K range

and averaged. The EXAFS spectra were extracted using the Athena software,[35] and data analysis was performed using Winxas.[36] For the fitting procedure, the amplitude and phase shift functions were calculated by FEFF 8.2.[37] Input files were generated by Atoms[38] within Artemis. The uncertainties of the distances and coordination numbers found by EXAFS are, respectively, 1% and 25%.

Theoretical Methods. Dispersion-corrected DFT calculations were performed with the Spartan'20 software packages[39,40] using the Becke three-parameter Lee−Yang−Parr exchange correlation functional (B3LYP),[41,42] the 6-31G* (LANL2DZ > Kr) basis set,[43] and the D3 dispersion correction.[44] The B3LYP/6-31G* method has been used for the optimization of the geometry of Tc and Re complexes.[45,46] The initial geometries were constructed using the Spartan graphical model builder, and conformational analysis was done using the Merck molecular force field. The lowest energy conformer was used as the starting geometry for the DFT calculations. All geometries were optimized without any symmetry constraints.

Other Techniques. UV−visible spectra were recorded at room temperature in a quartz cell (1 cm) on a Cary 6000i double-beam spectrophotometer. For the measurement, the samples were diluted with HDBP [30% (v/v)] in *n*-dodecane, which was also used as the reference baseline.

■ ASSOCIATED CONTENT

Data Availability Statement

All data generated or analyzed during this study are included in this published article and its Supporting Information files.

Ⓢ Supporting Information

The Supporting Information is available free of charge at https://pubs.acs.org/doi/10.1021/acsomega.4c00393.

Atomic coordinates for the structures of cis-Tc-$(NO_3)_2(DBP)_2(HDBP)_2$, trans-Tc-$(NO_3)_2(DBP)_2(HDBP)_2$, mer-Tc$(NO_3)_3(DBP)$-$(HDBP)_2$, (fac-Tc$(NO_3)_3(DBP)(HDBP)_2$), and Tc-$(NO_3)_3(DBP)$; XANES and UV−visible spectra of samples L and H; and calculated UV−visible spectra for cis-Tc$(NO_3)_2(DBP)_2(HDBP)_2$, trans-Tc-$(NO_3)_2(DBP)_2(HDBP)_2$, mer-Tc$(NO_3)_3(DBP)$-$(HDBP)_2$, and fac-Tc$(NO_3)_3(DBP)(HDBP)_2$) (PDF)

■ AUTHOR INFORMATION

Corresponding Author

Frederic Poineau − *Radiochemistry Program, University of Nevada Las Vegas, Las Vegas, Nevada 89154, United States;* ⓞ orcid.org/0000-0002-9517-2264; Email: poineauf@unlv.nevada.edu

Authors

Jonathan George − *Radiochemistry Program, University of Nevada Las Vegas, Las Vegas, Nevada 89154, United States*

Ramsey Salcedo − *Ph.D. Program in Chemistry, Graduate Center of the City University of New York, New York, New York 10016, United States; Hunter College of the City University of New York, New York, New York 10065, United States; Lehman College of the City University of New York, Bronx, New York 10468, United States*

Rachel Greenberg − *Ph.D. Program in Chemistry, Graduate Center of the City University of New York, New York, New York 10016, United States; Hunter College of the City*

University of New York, New York, New York 10065, United States; Lehman College of the City University of New York, Bronx, New York 10468, United States

Hossam Elshendidi − *Ph.D. Program in Chemistry, Graduate Center of the City University of New York, New York, New York 10016, United States; Hunter College of the City University of New York, New York, New York 10065, United States; Lehman College of the City University of New York, Bronx, New York 10468, United States*

Donna McGregor − *Ph.D. Program in Chemistry, Graduate Center of the City University of New York, New York, New York 10016, United States; Lehman College of the City University of New York, Bronx, New York 10468, United States;* ⓞ orcid.org/0000-0002-7927-6696

Benjamin Burton-Pye − *Ph.D. Program in Chemistry, Graduate Center of the City University of New York, New York, New York 10016, United States; Lehman College of the City University of New York, Bronx, New York 10468, United States*

Lynn C. Francesconi − *Ph.D. Program in Chemistry, Graduate Center of the City University of New York, New York, New York 10016, United States; Hunter College of the City University of New York, New York, New York 10065, United States;* ⓞ orcid.org/0000-0001-6314-2899

Alena Paulenova − *School of Nuclear Science and Engineering, 100 Radiation Center, Oregon State University, Corvallis, Oregon 97331-5903, United States*

Artem V. Gelis − *Radiochemistry Program, University of Nevada Las Vegas, Las Vegas, Nevada 89154, United States;* ⓞ orcid.org/0000-0002-5487-1472

Complete contact information is available at:
https://pubs.acs.org/10.1021/acsomega.4c00393

Notes

The authors declare no competing financial interest.

■ ACKNOWLEDGMENTS

◼ REFERENCES

(1) Segrè, E.; Seaborg, G. T. Nuclear isomerism in element 43. *Phys. Rev.* **1938**, *54*, 772.

(2) Johnstone, E. V.; Yates, M. A.; Poineau, F.; Sattelberger, A. P.; Czerwinski, K. R. Technetium: the first radioelement on the periodic table. *J. Chem. Educ.* **2017**, *94*, 320−326.

(3) *Spent Fuel Reprocessing Options. "IAEA-TECDOC-1587."*; IAEA: Vienna, 2008. https://www-pub.iaea.org/MTCD/publications/PDF/te_1587_web.pdf.

(4) Lumetta, G. J.; Allred, J. R.; Bryan, S. A.; Hall, G. B.; Levitskaia, T. G.; Lines, A. M.; Sinkov, S. I. Simulant testing of a co-decontamination (CoDCon) flowsheet for a product with a controlled uranium-to-plutonium ratio. *Sep. Sci. Technol.* **2019**, *54*, 1977−1984.

(5) George, K.; Masters, A. J.; Livens, F. R.; Sarsfield, M. J.; Taylor, R. J.; Sharrad, C. A. A review of technetium and zirconium extraction into tributyl phosphate in the PUREX process. *Hydrometallurgy* **2022**, *211*, 105892.

(6) Boukis, N.; Kanellakopulos, B. The interaction of tetravalent technetium with dibutyl phosphoric acid. *Radiochim. Acta* **1990**, *49*, 141−146.

(7) Mincher, B. J.; Modolo, G.; Mezyk, S. P. Review Article: The Effects of Radiation Chemistry on Solvent Extraction: 1. Conditions in Acidic Solution and a Review of TBP Radiolysis. *Solvent Extr. Ion Exch.* **2009**, *27*, 1−25.

(8) May, I.; Taylor, R. J.; Wallwork, A. L.; Hastings, J. J.; Fedorov, Y. S.; Zilberman, B. Y.; Mishin, E. N.; Arkhipov, S. A.; Blazheva, I. V.; Poverkova, L. Y.; Livens, F. R.; et al. The influence of dibutylphosphate on actinide extraction by 30% tributylphosphate. *Radiochim. Acta* **2000**, *88*, 283−290.

(9) Guedon, V.; Thieblemont, J. C.; Revel, Y.; Vandrot, A. Etude de la Précipitation des Produits de Fission ou de Corrosion sous l'Effet de la Dégradation Radiolytique du Solvent de Retraitement. *J. Nucl. Sci. Technol.* **1994**, *31*, 48−61.

(10) Miyake, C.; Hirose, M.; Yoshimura, T.; Ikeda, M.; Imoto, S.; Sano, M. "The third phase" of extraction processes in fuel reprocessing, (I) formation conditions, compositions and structures of precipitates in Zr-degradation products of TBP systems. *J. Nucl. Sci. Technol.* **1990**, *27*, 157−166.

(11) Vasudeva Rao, P. R.; Kolarik, Z. A review of third phase formation in extraction of actinides by neutral organophosphorus extractants. *Solvent Extr. Ion Exch.* **1996**, *14*, 955−993.

(12) Durain, J.; Bourgeois, D.; Bertrand, M.; Meyer, D. Comprehensive studies on third phase formation: application to U(VI)/Th(IV) mixtures extracted by TBP in N-dodecane. *Solvent Extr. Ion Exch.* **2019**, *37*, 328−346.

(13) Suresh, A.; Srinivasan, T. G.; Rao, P. R. V. Parameters influencing third-phase formation in the extraction of $Th(NO_3)_4$ by some trialkyl phosphates. *Solvent Extr. Ion Exch.* **2009**, *27*, 132−158.

(14) Chiarizia, R.; Jensen, M. P.; Borkowski, M.; Ferraro, J. R.; Thiyagarajan, P.; Littrell, K. C. Third phase formation revisited: the U(VI), HNO_3−TBP, n-dodecane system. *Solvent Extr. Ion Exch.* **2003**, *21*, 1−27.

(15) Plaue, J.; Gelis, A.; Czerwinski, K. Actinide third phase formation in 1.1 M TBP/nitric acid/alkane diluent systems. *Sep. Sci. Technol.* **2006**, *41*, 2065−2074.

(16) Kumar, S.; Koganti, S. B. Speciation studies in third phase formation: U(IV), Pu(IV), and Th(IV) third phases in TBP systems. *Solvent Extr. Ion Exch.* **2003**, *21*, 547−558.

(17) Chiarizia, R.; Jensen, M. P.; Rickert, P. G.; Kolarik, Z.; Borkowski, M.; Thiyagarajan, P. Extraction of zirconium nitrate by TBP in n-octane: Influence of cation type on third phase formation according to the "sticky spheres" model. *Langmuir* **2004**, *20*, 10798−10808.

(18) Antonio, M. R.; Ellis, R. J.; Estes, S. L.; Bera, M. K. Structural insights into the multinuclear speciation of tetravalent cerium in the tri-n-butyl phosphate−n-dodecane solvent extraction system. *Phys. Chem. Chem. Phys.* **2017**, *19*, 21304−21316.

(19) Zhang, P.; Kimura, T. Complexation of Eu (III) with dibutyl phosphate and tributyl phosphate. *Solvent Extr. Ion Exch.* **2006**, *24*, 149−163.

(20) George, J.; Salcedo, R.; Greenberg, R.; Elshendidi, H.; McGregor, D.; Burton-Pye, B.; Francesconi, L. C.; Paulenova, A.; Gelis, A. V.; Poineau, F. Structural investigation of technetium dibutylphosphate species using x-ray absorption fine structure spectroscopy. *Inorg. Chem.* **2023**, *62*, 16378−16387.

(21) Vasilchenko, D.; Vorobieva, S.; Baidina, I.; Piryazev, D.; Tsipis, A.; Korenev, S. Structure and properties of a rhodium (III) pentanitrato complex embracing uni-and bidentate nitrato ligands. *Polyhedron* **2018**, *147*, 69−74.

(22) Steed, J. W.; Tocher, D. A. Nitrato complexes of ruthenium (IV): chelating,"semi-chelating" and monodentate coordination modes. *Polyhedron* **1994**, *13*, 167−173.

(23) Kostin, G. A.; Nikiforov, Y. A.; Kuratieva, N. V. Synthesis and structure of ruthenium nitroso complexes with nitrate anions and pyridine as ligands. *J. Struct. Chem.* **2020**, *61*, 86−94.

(24) Wickleder, M. S.; Gerlach, F.; Gagelmann, S.; Bruns, J.; Fenske, M.; Al-Shamery, K. Thermolabile noble metal precursors:$(NO)[Au(NO_3)_4]$,$(NO)_2[Pd(NO_3)_4]$, and $(NO)_2[Pt(NO_3)_6]$. *Angew. Chem., Int. Ed.* **2012**, *51*, 2199−2203.

(25) Morozov, I. V.; Palamarchuk, D. M.; Kozlovsky, V. F.; Troyanov, S. I. Synthesis and crystal structure of oxonitrate complexes $Cs[VO_2(NO_3)_2]$, $Cs[MoO_2(NO_3)_3]$, and $MoO_2(NO_3)_2$. *Crystallogr. Rep.* **2010**, *55*, 386−392.

(26) Wilson, A. M.; Bailey, P. J.; Tasker, P. A.; Turkington, J. R.; Grant, R. A.; Love, J. B. Solvent extraction: the coordination chemistry behind extractive metallurgy. *Chem. Soc. Rev.* **2014**, *43*, 123−134.

(27) Lamouroux, C.; Moulin, C.; Tabet, J. C.; Jankowski, C. K. Characterization of zirconium complexes of interest in spent nuclear fuel reprocessing by electrospray ionization mass spectrometry. *Rapid Commun. Mass Spectrom.* **2000**, *14*, 1869−1877.

(28) Hardy, C. J.; Scargill, D. Studies on mono-and di-n-butylphosphoric acids-III The extraction of zirconium from nitrate solution by di-n-butylphosphoric acid. *J. Inorg. Nucl. Chem.* **1961**, *17*, 337−349.

(29) Weck, P. F.; Kim, E.; Poineau, F.; Rodriguez, E. E.; Sattelberger, A. P.; Czerwinski, K. R. Technetium (IV) halides predicted from first-principles. *Inorg. Chem.* **2009**, *48*, 6555−6558.

(30) Moffat, A. J.; Thompson, R. D. *Basic Studies of Chemical Stability in Extraction Systems. i. The Effect of Zirconium Nitrate and Nitric Acid Upon the Chemical Stability of Tributyl Phosphate (No. IDO-14543)*; Phillips Petroleum Co. Atomic Energy Div.: Idaho Falls, ID, 1961.

(31) Uetake, N. Precipitation formation of zirconium-dibutyl phosphate complex in purex process. *J. Nucl. Sci. Technol.* **1989**, *26*, 329−338.

(32) Motokawa, R.; Kobayashi, T.; Endo, H.; Mu, J.; Williams, C. D.; Masters, A.; Antonio, M. R.; Heller, W. T.; Nagao, M. A telescoping view of solute architectures in a complex fluid system. *ACS Cent. Sci.* **2018**, *5*, 85−96.

(33) Yang, X.; Xu, L.; Zhang, A.; Xiao, C. Organophosphorus Extractants: A Critical choice for actinides/lanthanides separation in nuclear fuel cycle. *Chem.—Eur. J.* **2023**, *29*, No. e202300456.

(34) Graham, T. R.; Castillo, J.; Sinkov, S.; Gelis, A. V.; Lumetta, G. J.; Cho, H. Multiplicity of Th(IV) and U(VI) HEH[EHP] chelates at low temperatures from concentrated nitric acid extractions. *Inorg. Chem.* **2023**, *62*, 792−801.

(35) Ravel, B.; Newville, M. ATHENA,ARTEMIS,HEPHAESTUS: data analysis for X-ray absorption spectroscopy using*IFEFFIT*. *J. Synchrotron Radiat.* **2005**, *12*, 537−541.

(36) Ressler, T. WinXAS: a program for X-ray absorption spectroscopy data analysis under MS-Windows. *J. Synchrotron Radiat.* **1998**, *5*, 118−122.

(37) Rehr, J. J.; Albers, R. C. Theoretical approaches to x-ray absorption fine structure. *Rev. Mod. Phys.* **2000**, *72*, 621−654.

(38) Ravel, B. ATOMS: crystallography for the X-ray absorption spectroscopist. *J. Synchrotron Radiat.* **2001**, *8*, 314−316.

(39) Shao, Y.; Molnar, L. F.; Jung, Y.; Kussmann, J.; Ochsenfeld, C.; Brown, S. T.; Gilbert, A. T.; Slipchenko, L. V.; Levchenko, S. V.; O'Neill, D. P.; DiStasio, R. A., Jr.; et al. Advances in methods and algorithms in a modern quantum chemistry program package. *Phys. Chem. Chem. Phys.* **2006**, *8*, 3172−3191.

(40) Spartan 20 from Wavefunction, Inc.. 18401 Von Karman Avenue, Irvine, CA 92612. 2023, www.wavefun.com.

(41) Lee, C.; Yang, W.; Parr, R. G. Development of the Colle-Salvetti correlation-energy formula into a functional of the electron density. *Phys. Rev. B: Condens. Matter Mater. Phys.* **1988**, *37*, 785−789.

(42) Becke, A. D. Density-functional thermochemistry. III. The role of exact exchange. *J. Chem. Phys.* **1993**, *98*, 5648−5652.

(43) Hay, P. J.; Wadt, W. R. Ab initio effective core potentials for molecular calculations. Potentials for K to Au including the outermost core orbitals. *J. Chem. Phys.* **1985**, *82*, 299−310.

(44) Grimme, S.; Hansen, A.; Brandenburg, J. G.; Bannwarth, C. Dispersion-corrected mean-field electronic structure methods. *Chem. Rev.* **2016**, *116*, 5105−5154.

(45) Qiu, L.; Lin, J. G.; Gong, X. D.; Ju, X. H.; Luo, S. N. Theoretical Studies on Electronic Structure and Absorption Spectrum of Prototypical Technetium-Diphosphonate Complex [99m] Tc-MDP. *Bull. Korean Chem. Soc.* **2011**, *32*, 2358−2368.

(46) Santoro, G.; Zlateva, T.; Ruggi, A.; Quaroni, L.; Zobi, F. Synthesis, characterization and cellular location of cytotoxic constitutional organometallic isomers of rhenium delivered on a cyanocobalmin scaffold. *Dalton Trans.* **2015**, *44*, 6999−7008.